Egypt. J. Chem. **Vol. 63,** No. 4, pp. 1397 - 1409 (2020)

Egyptian Journal of Chemistry
http://ejchem.journals.ekb.eg/

Removing Tramadol Hydrochloride from Wastewater Using Kaolinite Nanocomposite

M. Farouk[1], A. S. Amin[2]*, M. A. Diab[3], Adel Z. El-Sonbati[3], M. S. Ibrahime[4]
[1]*Reference laboratory, Holding Company for Water and Wastewater, Cairo, Egypt.*
[2]*Chemistry Department, Faculty of Science, Banha University, Banha, Egypt.*
[3]*Chemistry Department, Faculty of Science, Damietta University, Damietta, Egypt.*
[4]*Environment Department, Faculty of Science, Damietta University, Damietta, Egypt.*

PHARMACEUTICALS are classified as emerging environmental pollutants that have a potential harmful impact on environment and human health. This study aims to treat the tramadol hydrochloride (TH) in different water resources in Egypt. The identification and quantification of TH was explored using LC/MS/MS instrument. The study proposed kaolinite/ZnO nanocomposite (K/ZnO) as a new solution for TH treatment. The characterization study showed that the highest photodegradation activity was achieved in the case of K/ZnO40%. The photodegradation kinetics and thermodynamics are investigated. The obtained results reveal that Pseudo-first order model is well fitted with a correlation coefficient (0.990). Moreover, the positive values of ΔH° and ΔS° show that the photodegradation process is an endothermic reaction. Positive value of free energy indicates that the adsorption process is not spontaneous.

Keywords: Kaolinite, Tramadol hydrochloride, Photocatalyst, Thermodynamic, Reaction kinetic

Introduction

In the (heterogeneous) photocatalysis oxidation process, organic pollutants are destroyed in the presence of semiconductor photocatalysts to give CO_2 and H_2O (e.g., TiO_2, WO_3, ZnO, and Fe_2O_3.) **[1].** Zinc oxide (ZnO) has been studied extensively because of its low-cost semiconductor, high activity, desirable physical and chemical properties, availability, high quantum efficiency, nontoxicity exhibit and having large band gap ~ 3.3 eV **[2]**. ZnO nanoparticles (NPs) can be prepared via various methods (hydrothermal synthesis) **[3,4]** coprecipitation method**[5,6]**, sol–gel method**[7,8]**, non-aqueous solution method**[9]**, photolysis**[10]**, solid state mixing of precursors**[11]**, thermal decomposition of precursor**[12]**, microwave assisted synthesis**[13]**, vapor deposition techniques**[14]**. Unfortunately, ZnO is a toxic compound, for this reason ZnO should be loaded over solid matrices such as kaolinite clay to restrict the movement of ZnO NPs but not suppressing their unique properties. Pure kaolinite ($Al_2O_3/2SiO_2/2H_2O$) is white in color and its chemical composition is 46.54% SiO_2, 39.50% Al_2O_3 and 13.96% H_2O. It is used in wide industrial applications in the production of ceramics, porcelain, and filler for paint, rubber, and plastics **[15]**. Based on its low cost, non-toxicity, high surface area and large potential for ion exchange, resulting from a net negative charge on the structure of the minerals **[17,18]** kaolinite was used for the preparation of ZnO-based nanocomposites**[2,13]**. Rakic´ et al. used Clinoptilolite, bentonite and kaolin in adsorption of salicylic acid, acetylsalicylic acid and atenolol from aqueous solutions **[33],** also Hong et al. used Kaolinite in removal of ciprofloxacin from aqueous solutions **[32].** Tramadol Hydrochloride (TH) is a centrally acting analgesic agent, is used in the treatment of mild to moderate pain. It has been approved for use in the United States since 1995 and in France since 1997. It has a low affinity to opioid receptors and inhibits the reuptake of norepinephrin and serotonin making a significant contribution to analgesic performance by blocking nociceptive impulses in the spine. Its analgesic effect is partially blocked by naloxone, but totally blocked by yohimbine. Tramadol is

*Corresponding author e-mail: mohamedfaroukmoustafa@gmail.com. Tel. 01284444391
Received 24/7/2019; Accepted 14/09/2019
DOI: 10.21608/ejchem.2019.15204.1924

rapidly absorbed orally and has a distribution volume of 3.0 L kg^{-1}. Following a 100 mg oral dose, a peak concentration of approximately 0.3 mg L^{-1} is detected in 2h **[18]**. post-dose. After a single bolus infusion of 100 mg tramadol, concentrations in plasma can be immediately detected. Elimination is slow and characterized by an elimination half-life of 5.0–6.0 h. According to physicochemical properties of tramadol, its effect is expected to remain mainly in the water phase. The water solubility of tramadol is relatively high and its volatilization from the water phase into air is negligible. The reason behind that is related to the low Henry coefficients which equal to ($1.54x10^{-11}$atm m^{-3} mol^{-1}) at 25° C. Furthermore, its n-octanol/water partition coefficients log K_{ow} (3.01) indicates a tendency to remain in the water phase instead of accumulation in sewage sludge or in aquatic organisms. Thus, it is quite difficult to treat by traditional treatment process as proposed in **[19]**.Tramadol has been detected in effluents from wastewater treatment plants (WWTPs), in some rivers and lakes in both Europe and North America. A report from Eawag (German acronym for the Swiss Federal Institute of Aquatic Science and Technology) indicates the presence of Tramadol at various locations in Lake Constance, Switzerland, at concentrations of 0.009 µg L^{-1} **[20]**. Kasprzyk-Hordern et al. detected tramadol at concentrations up to 7.0 µg L^{-1} in rivers of South-Wales, UK, impacted by treated wastewater discharges **[21]**. In addition, Rúa-Gómez and Püttmann reported the presence of tramadol in German rivers at concentration of 0.025 to 0.381 µg L^{-1}**[19]**. However, researchers found that tramadol may produce significant neurologic toxicity, including seizures, Lethargy, Agitation, Dizziness, Seizures, Confusion, Ataxia, Diplopia, coma and respiratory depression, as well as mild tachycardia and hypertension **[22]**. As results, the removal of tramadol from water is necessary and could be considered as a vital issue in water treatment plants. So that this study aimed to remove TH from water using K/ZnO nanocomposite.

Materials and Methods

Materials

Kaolin was purchased from El Nasr mining company. TH was obtained from (Sintex Technology- London-England). Ammonia solution 30%, Potassium phosphate dibasic and potassium phosphate monobasic were purchased from panreac. Methanol 99.9% was obtained from Sigma. Zinc sulfate was obtained from (El-Nasr pharmaceutical chemical Company). LC/MS/MS instrument from Waters, pH from Hach, FTIR from Bruker and RDX & X-ray Analysis from JEOL.

Methods

Preparation of ZnO/kaolinite nanocomposite

K/ZnO nanocomposite was synthesized from intercalation of ZnO with thermal activated kaolinite. Kaolin activation was done thermally at 750°C for 2 hrs using electrical muffle furnace. ZnO nanoparticle was prepared by adding 100 ml of 0.2 M solution of $ZnSO_4$ in conical flask and aqueous ammonia solution 25% was added drop wise with constant rate 5ml/min with stirring until the pH of the solution reached to 10. The obtained precipitate was filtrated on a Buckner funnel and washed several times with deionized water and methanol. The precipitate was dried in oven at 70°C for 8 hrs and calcined at 500°C in a muffle furnace for 2 hrs. To prepare different ratio of ZnO/Kaolinite, (2, 6 and 8g) of ZnO powder mixed with 20g kaolinite in 100ml deionized water for 24hrs to obtain K/ZnO (K/ZnO 20%, K/ZnO 30% and K/ZnO 40%) nanocomposite with ratio 20%, 30% and 40% respectively, then composites filtered and washed several times by deionized water and methanol. The composites were dried in an oven at 80°C for 2hrs and calcined at 700°C in a muffle furnace for 2 hrs.

Preparation of TH solutions

250 mg of TH were dissolved in 250 ml methanol to prepare 1000 mg L^{-1} stock solution. Working standard was prepared by direct dilution of stock solution using methanol to prepare 10 mg L^{-1}. Series of standards solutions were prepared for both instrument calibration and batch experiments in milli-Q deionized water.

Instrumentation

pH meter model (Hach, Sension1) equipped with reference electrode used to adjust the solutions pH, Rotor shaker 15 position model (THERMO, SHKE2000) equipped with timer used to batch experiments, (LC/MS/MS) ultra-performance liquid chromatography (Acquity UPLC) equipped with mass selective detector (Xevo -TQS) used to quantification of TH in the aqueous phase. Each sample before analysis was centrifuged at 6000 rpm for 15 min to remove fine kaolinite particles, then 10 µl aliquot was injected (direct injection) into a reverse phase UPLC column C8 (1.7µm*2.1*50mm). Separation of

the analytes was achieved using gradient eluent conditions with a mixture of (A) water and (B) methanol HPLC grade. Eluent gradient started by 90% (A) in the first 2.5 min, 10% (A) from 2.5 to 7.75 min, 100% (B) from 7.75 to 8.50 min and then backed to 90% (A) from 8.5 to 10 min. The flow rate was 0.450 ml min^{-1}, after elution from the UPLC column, the analytes were detected by MS/MS detector using Electron-Spray-ionization (ESI) in positive mode with the following conditions, 264.1(m/z) parent ion was fragmented into 58(m/z) daughter ion by 11 volt collision energy, 20V cone volt, 450 ˚C dessolvation temperature, 800 Lhr^{-1} dessolvation, 150 L hr^{-1} Cone and 7.0 bar Nebulize (r). Each batch controlled by calibration curve, Lab Control Sample (LCS) and reagent water blanks. Calibration curve consists of five points from 0.005 to 1 µg L^{-1} to cover drinking water samples concentration and lab control sample (LCS) concentration was 2.0 µg L^{-1} to check LC/MS/MS instrument performance. Reagent water blanks to control cross contamination during sample preparation blank concentration should be less than limit of quantification (LOQ) (0.05 µg L^{-1}).

Characterization methods

Fourier transforms infrared spectroscopy

A Bruker-Vertex 70 spectrometer in the range 4000 - 400 $cm^{-1}$was used to obtain the FTIR spectrum that were used to study the surface chemistry of the absorbent. The samples were mixed with potassium bromide and the mixtures were pressed into pellets before analysis

Energy Dispersive X-ray Analysis:

Elemental composition of each modified kaolinite was analyzed by EDX (JEOL, JSM-6390LA), with the following conditions accelerating voltage 15 K.V, magnification power 50x and resolution (512*384).

Scanning electron microscope (SEM):

The material properties, surface and compositional images of the kaolinite were defined by (JEOL, JSM-6390LA) with accelerating voltage 15 K.V, magnification power up to 500x. The samples were covered by a thin filament of gold to improve conductivity during examination by SEM.

Evaluation of photodegradation activity

In order to investigate the optimum photodegradation activity of resulting composite, Batch experiment was performed at room temperature by adding a known amount of (K/ZnO20%, K/ZnO30% or K/ZnO40%) to 50 ml of 20mg L^{-1} Malachite green solution into number of 100 ml conical flasks sealed with aluminum foil on a rotary shaker at 250 rpm for 15 minuet in dark followed by 30min in solar light.

Adsorption batch experiments

The batch experiments were carried out to study the optimum conditions of TH removal, such as solution pH, nanocomposite dose (K/ZnO 40%), TH initial concentration, contact time, ionic strength and reaction temperature. Photodegradation batch technique was studied by shaking a suitable amount of (K/ZnO 40%) with a solution of TH for 15 min in dark place then shaking in solar light for 30 min at 250 rpm. The effect of pH was conducted by adding 0.1 g of (K-ZnO40%) to 50 ml of 10 µg L^{-1} TH solution at different pH values (3.0 to 9.0) which adjusted by phosphate buffer solution and 0.1 M HCl or 0.1 M NaOH. The effect of adsorbent dosage was conducted by adding desired amounts of K-ZnO 40% (0.01, 0.02, 0.05, 0.1, 0.2, 0.3, 0.5 and 1.0 g) to 50 ml of 10 µg L^{-1} TH solutions at the optimum pH value. To investigate the effect of TH concentration, experiments were carried out by adding 0.2g of K-ZnO40% to 50ml of TH solutions at concentrations (0.005, 0.01, 0.02, 0.05, 0.1, 0.8, 2.0, 4.0, 8.0, and 16 mg L^{-1}) at optimal pH values. Equilibrium time was conducted by adding 0.2 g K-ZnO 40% to 12 mg L^{-1} TH solutions at different durations of (5, 15, 30, 45, 60, 90, 120, 150, 210 and 300 min). To investigate the effect of thermodynamics the experiments were carried out at optimum conditions of pH, TH concentration and K-ZnO 40% dosage at equilibrium time. To investigate the effect of ionic strength, experiments were carried out at different concentrations of $CaCl_2$ (0.01, 0.05, 0.1, 0.3, and 0.5 M) at optimum conditions that mentioned previously.

Result and Discussion

Characterization of K/ZnO

Fourier transforms infrared spectroscopy results

The FT-IR spectrum of the raw kaolin was performed to show the typical bands of these materials. A band assigned to water OH stretching is found at 3485 cm^{-1}, with the band of the stretching of OH group coordinated to the octahedral cations at 3625 cm^{-1} .The water bending band is observed at 1619 cm^{-1}. In the region of low wavenumbers, there are up to 4 characteristic

bands of this mineral; 795 (free silica and/or quartz admixtures, always present in raw kaolin), 753 (Si-O-Al), 652 (Si-O out-of-plane bending), and 536 (Si-O-Al bending, Al octahedral). While in case of K-ZnO as in **Fig. 1a**, a band assigned to water OH stretching has been detected at 3451 cm^{-1} while water bending band has been observed at 1619 cm^{-1}. The band observed at 2921 cm^{-1} is attributed to C-H stretching. Between 1200 and 400 cm^{-1}, bands corresponding to silica could be observed, which represented in 3 characteristic bands (693 and 788 cm^{-1} for Si-O quartz and 662 cm^{-1} for Si-O-Si bending). The bands between 450 and 600 cm^{-1} are correlated to metal oxide bond Zn-O **[23]**.

SEM study

It could be indicated from the SEM results in Fig. 2 that the morphology of clays–ZnO nanocomposites could be altered substantially by increasing the amount of loaded ZnO**.**

Elemental analysis

Table 1 reveals that further increase in the percentage of ZnO will decrease the percentage of SiO_2. This reflects that the percentage of Al_2O_3 leached out from the structure and the amount of ZnO loaded could be increased.

Photodegradation activity

As shown in **Fig. 3** the highest photodegradation activity was reached in the case of K-ZnO40%. This is may be related to increase the amount of ZnO loaded over kaolinite surface that could be enhance the amount of catalyst exposed to solar light and increase the photoderadation activity.

Removing Tramadol Hydrochloride Using K/ZnO nanocomposites

Effect of pH

The effect of pH on the photocatalytic degradation rate of organic compounds is realized as a complex issue because these variations can modify the electrostatic interactions between the catalyst surface and substrate molecules. In addition, the formation of hydroxyl radicals by the reaction is found between the hydroxide ions/H_2O and the generated positive holes in the catalyst surface. The surface charge of ZnO could change from positive to negative value as pH increases at values higher than the point of zero charge. It has been reported to be 9.3 for ZnO in **[24]**. Moreover, depending on the ionic form of the substrate (anionic or cationic) electrostatic attraction or repulsion between the catalyst's surface and the organic molecule is taking place and consequently enhances or inhibits respectively, the photodegradation rate. TH presents a pKa value of 9.23 **[25]**. According to the inset of **Fig. 4**, an increase is observed by moving from acidic pH 3 to basic pH values at pH 9. At very acidic pH, the tertiary amine group and the hydroxyl group of TH can be protonated whereas the catalyst surface is also positively charged. Thus, repulsion between the catalyst and the molecules of TH is taking place and consequently it hinders the photocatalytic degradation. In addition to this, the particles of the catalyst might tend to agglomerate under acidic conditions, thus the surface area available for drug adsorption and photon adsorption decreased. Furthermore, although that positive hole is considered to contribute more in the photocatalytic oxidation at low pH, it is reported that for structurally related compounds to TH the photogenerated holes participate in a minor extent in the degradation, while $^{\bullet}OH$ are the main reactive species **[26]**, but their formation is less favored at acidic pH media. Increasing gradually the pH till values pH was 9 around the pKa of TH lead to a progressive decrease of TH protonation while for pH above the pH_{pzc} of ZnO the surface of the catalyst was negatively charged, thus and attraction of TH to catalyst's surface took place increasing the photocatalytic rates. Additionally, the increase of OH concentration at alkaline pH leads to higher generation of $^{\bullet}OH$ and thus to the enhancement of the degradation rate. This result confirmed by Lambropoulou et al. concluded that, higher degradation rates of venlafaxine using TiO_2/UV were obtained at alkaline conditions pH10 **(26).**

Effect of catalyst amount

As shown in **Fig. 5**, it is obvious that the photodegradation rate increases with the increase of the catalyst's amount up to a level which corresponds to the optimum activation of the catalyst particles by the incident light. In our case, this limit corresponded to maximum removal 86.8% is found at 0.2g/50ml of catalyst and the increase of the reaction rate that it is observed up to this amount level, is attributed to the increase of the photogenerated active sites in the catalyst surface and consequently the formation of greater amounts of $^{\bullet}OH$ and hole (h^+). However, above this limiting value, further increase of K-ZnO40% nanocomposite amounts leads to a reduction of the reaction rate due to the blocking of the solar light passage and the increase of the light-scattering by the suspended particles of the catalyst **[26]**. The

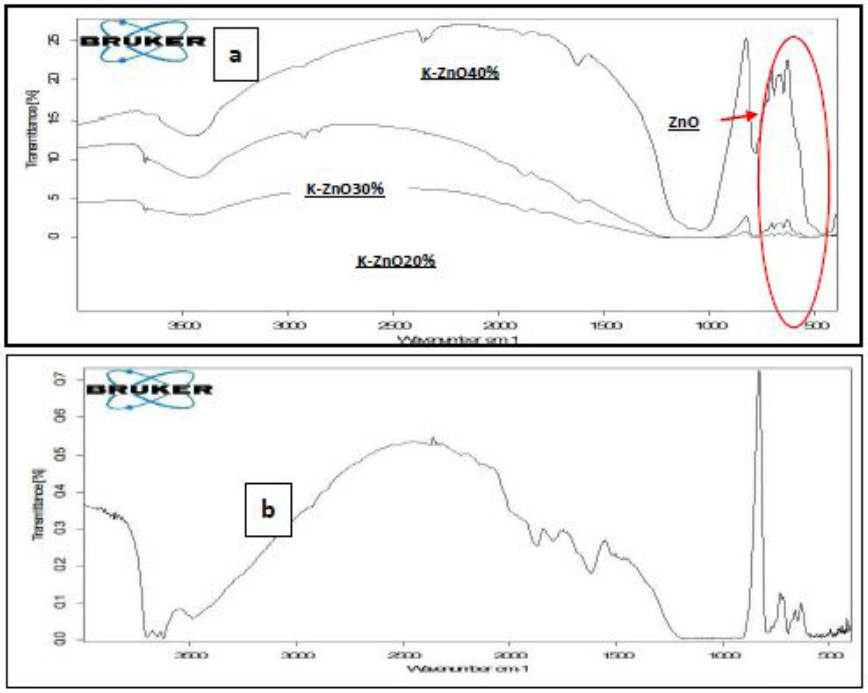

Fig. 1(a,b). FTIR spectra of kaolinite nanocomposite (K-ZnO) and Raw kaolin

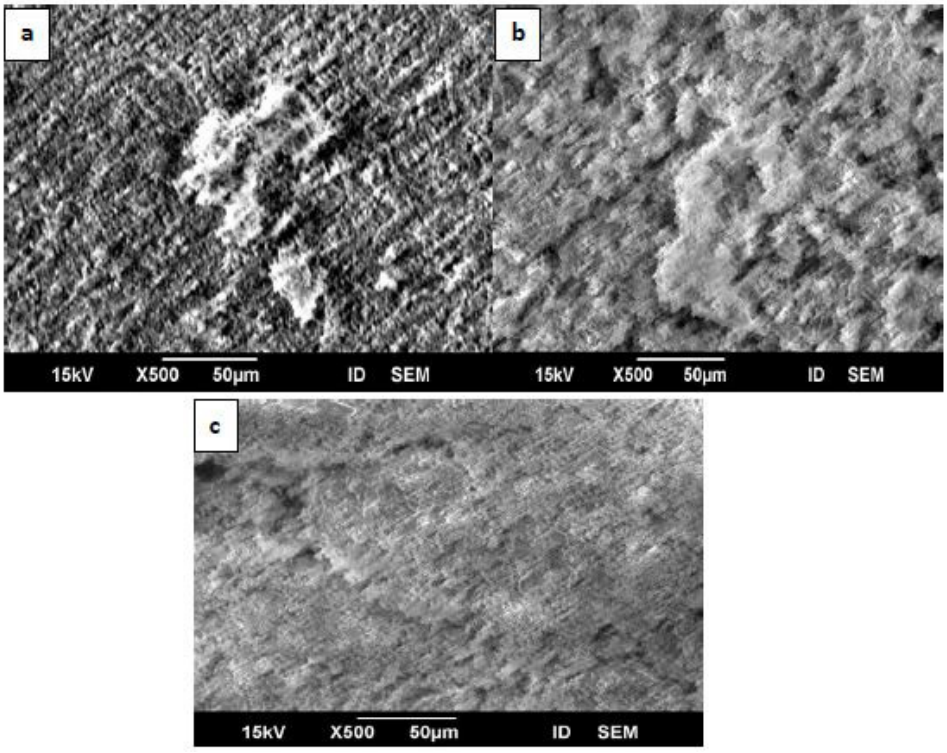

Fig. 2. SEM images of kaolinite that loaded by different percentages of ZnO a) K-ZnO 20% b) K-ZnO 30% c) K-ZnO 40%

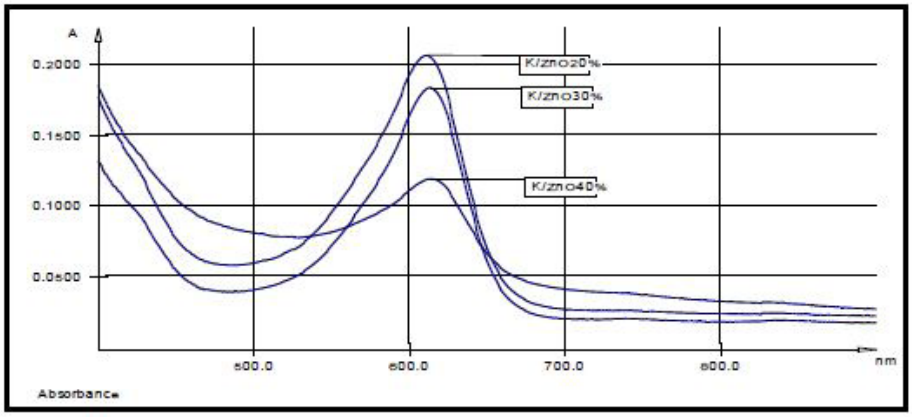

Fig. 3. The photodegradation activity of K-ZnO 20%, K-ZnO 30% and K-ZnO 40% for removing MG dye

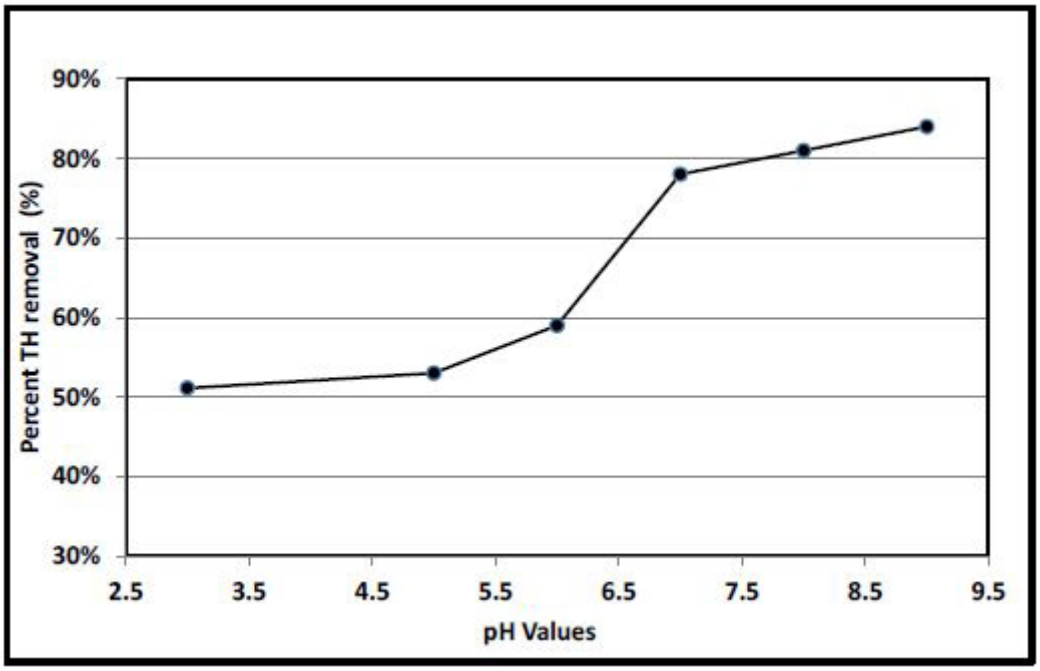

Fig. 4. Effect of pH on TH degradation, initial TH concentration 10 µg L^{-1}, clay dosage 0.1 g/50ml and contact time 15 min in dark then followed by 30 min in solar light.

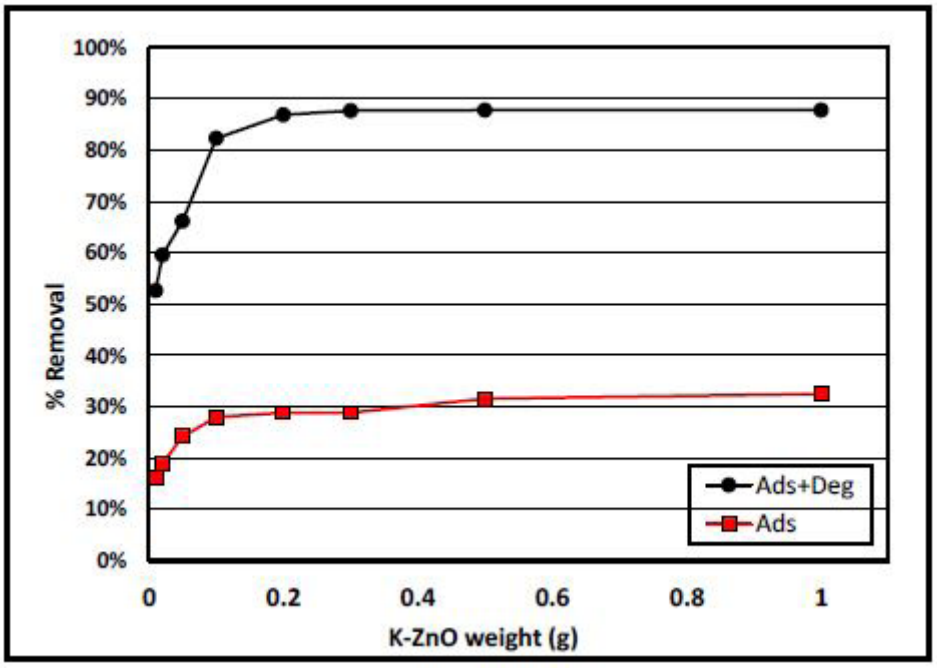

Fig. 5. Effect of K-ZnO amount on TH degradation, initial TH concentration 10 µg L^{-1}, pH 9 and contact time 15 min in dark then followed by 30 min in solar light.

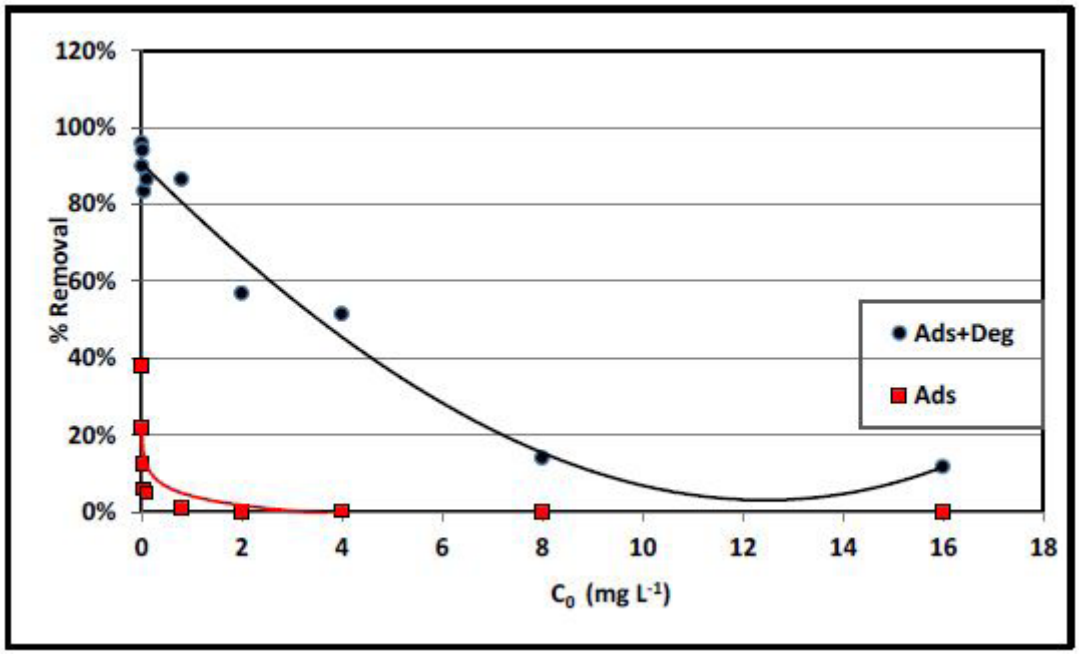

Fig. 6. Effect of initial TH concentration on degradation process, K-ZnO40% amount 0.2g/50ml, at pH 9 and contact time 15 min in dark then followed by 30 min in solar light.

limiting value of the catalyst amount depends on the geometry of the reactor and the working conditions. Furthermore, the decrease of the reaction rates at high catalyst amount are due to other phenomena that may take place like agglomeration (particle–particle interactions) which result in a loss of surface area available for light harvesting **[27]**.

Effect of TH concentration

As shown in **Fig. 6**, the rate of removal is decreasing with the increase of the initial concentration of TH. As indicated in the inset of **Fig. 6**, the removal percentage decreases from 86.5% at 0.8 mg/l to 51.5% at 4 mg/l. This phenomenon is attributed to the fact that amounts of $^{\bullet}OH$ and hole (h^+) becomes the limiting reactant at increased TH concentrations. Moreover, at high substrate concentrations more photons could be absorbed by the parent compound or by the formed by-products and consequently K-ZnO40% activation could be reduced **[28]**.

Effect of agitation time

As shown in **Fig. 7**, adsorption experiment was performed at dark and TH concentration used was 12 mg L^{-1}, the amount of TH was removed less than 1.0%, which demonstrated that the adsorption of TH was negligible. The photolysis removal percentage of TH has been increased from 34.6% to 64.2% with increasing the agitation time from 25min to 225min as shown in the previous figure. This is due to the increase in the amount of $^{\bullet}OH$ and hole (h^+) by time increasing. This result has been confirmed by **Niu et al**. whose conclude that adsorption of sulfamethoxazole in dark by TiO_2 nanoparticle is found below 5% and the photolysis rate constants of sulfamethoxazole has increased with the increase in the photolysis time and the TiO_2 concentration**[29]**.

Photodegradation Kinetics

For realizing more data about the adsorption mechanism, different kinetic models are applied; pseudo-first- or pseudo-second-order reaction **Eq (1, 2)**

Pseudo first order:

$$\ln(q_e - q_t) = \ln q_e - k_1 t \quad (1)$$

Pseudo − second – order:

$$\frac{t}{q_t} = \frac{1}{k_2 q_e^2} + \frac{1}{q_e} t \quad (2)$$

Where (t) is the adsorption time, q_e and q_t, (mg g^{-1}) are the adsorbed amount of TH at equilibrium and time t and k_1, and k_2 are the rate constants of pseudo-first order and pseudo-second order, respectively.

Figure 8 shows the photodegradation kinetics of 12 mg L^{-1} TH under optimized conditions. The results showed good compliance with the first-order kinetic model in terms of higher correlation coefficients R^2 (0.990). This result has been confirmed by **Yang et al**., photocatalytic degradation of sulfachlorpyridazine, sulfapyridine and sulfisoxazole by TiO_2 compliance with the first-order kinetic model **[30]**.

Effect of ionic strength

The effect of calcium chloride on the photodegradation of TH by K-ZnO40% is shown in **Fig. 9**. When calcium chloride concentration has been increased from 0.01 to 0.10 mol $L^{-1}$the photodegradation percentage of TH increased from 37.7 to 70.07%. This is due to the partial neutralization of the positive charge on (K-ZnO40%) and the consequent compression of the electrical double layer by the Cl^- anion. The chloride ion could also enhance the adsorption of TH ion onto (K-ZnO40%) surface by pairing of their charges and hence reducing the repulsion between the TH molecules adsorbed on the surface. This initiates (K-ZnO40%) to adsorb more of positive TH ion that enhances the photodegradation of TH on the surface of K-ZnO. While at calcium chloride concentration from 0.1 to 0.5 mol L^{-1}, the photodegrdation percentage has increased only from 70.07% to 78.2%. The decrease in the rate of TH degradation is due to the presence of excess from chloride ions that scavenging hole and reduced photodegradation **[31].**

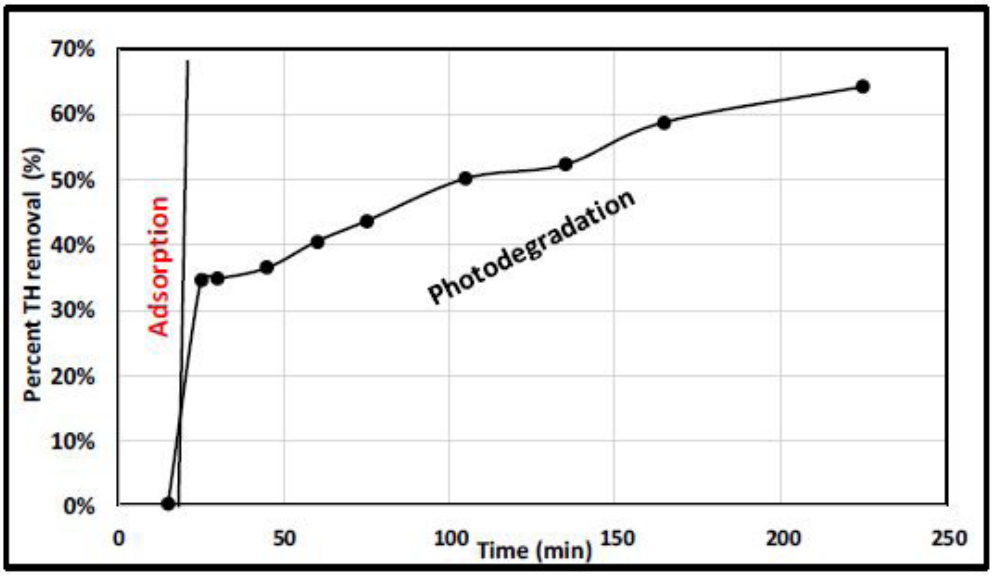

Fig. 7. Effect of agitation time on degradation of TH. Initial concentrations 12 mg/l and K-ZnO40% dose was 0.2g/50ml

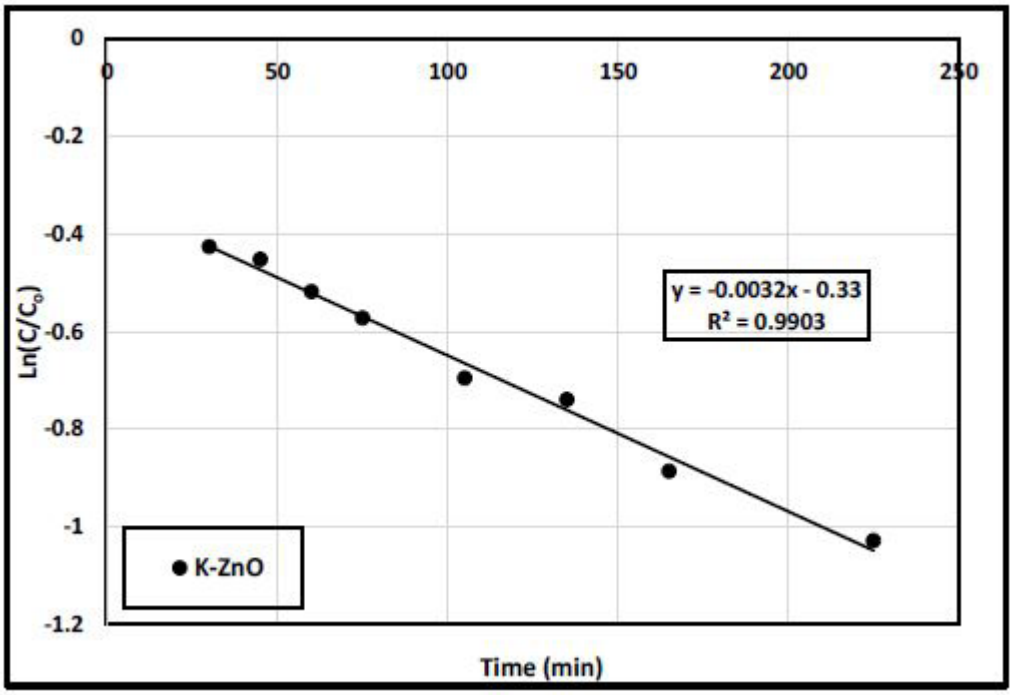

Fig. 8. Kinetic plots of pseudo first order for the photo degradation of TH by K-ZnO

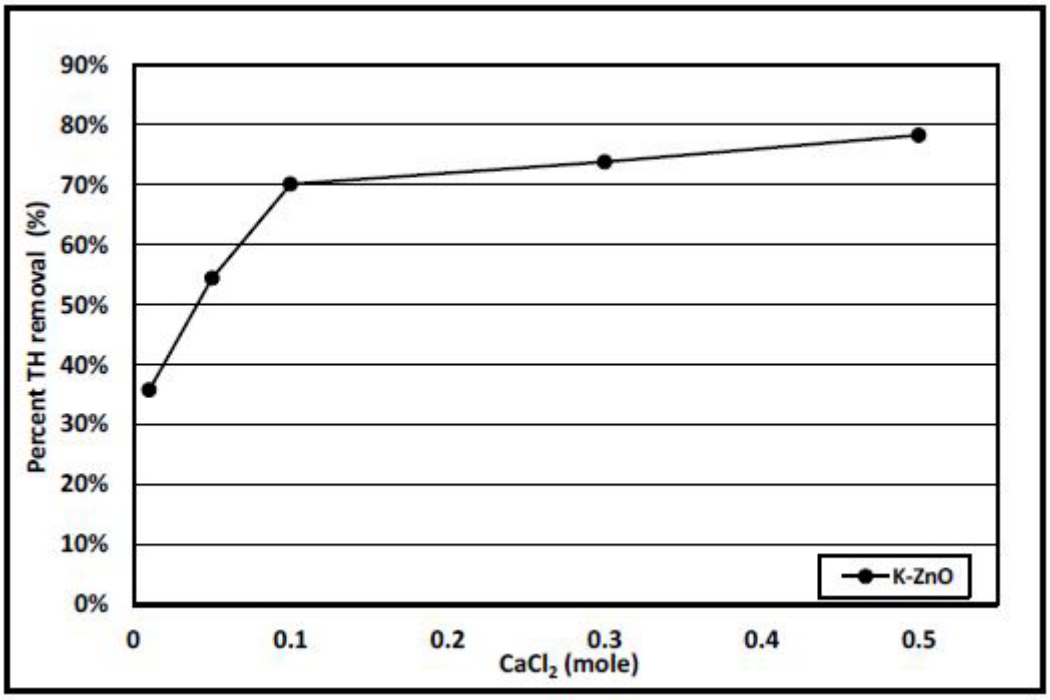

Fig. 9. Effect of ionic strength on degradation of TH at 12mg L-1 of TH, pH9, 0.2 g/50 ml K-ZnO40% and agitation time 30 min

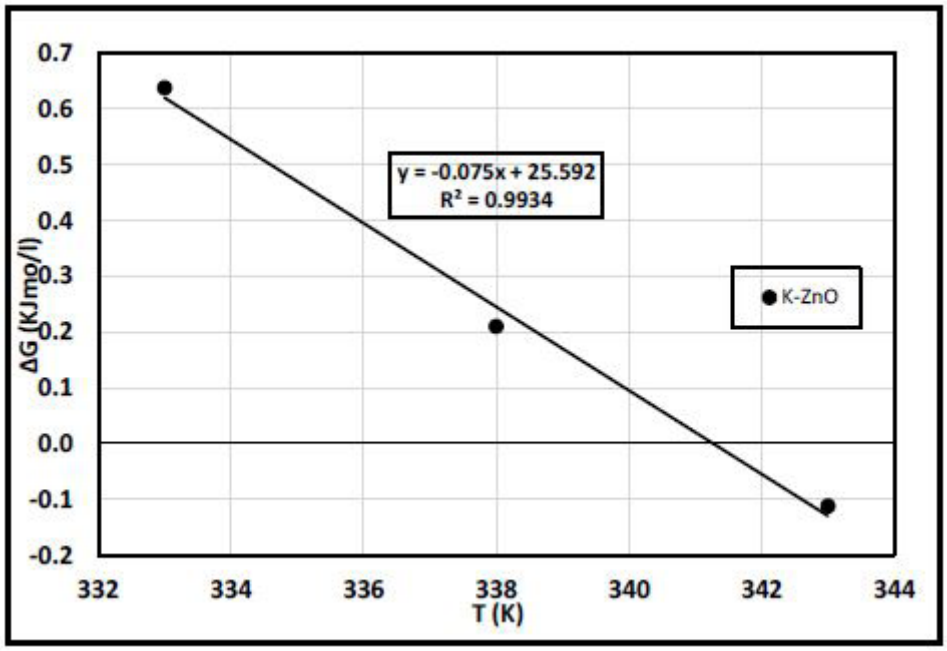

Fig. 10. Plots ΔG° versus T for photodegradation of TH by K-ZnO

TABLE 1. Chemical Composition, in Mass %, of the Natural Kaolin, K-ZnO 20%, K-ZnO 30% and K-ZnO 40%

CLAY	SiO_2	Al_2O_3	Fe_2O_3	MgO	K_2O	TiO_2	CaO	Na_2O	Cr_2O_3	ZnO
Raw Kaolin	68.1	26.5	___	1.33	1.83	___	___	2.15	___	___
K-ZnO20%	56.2	17.4	___	___	___	___	___	___	___	26.2
K-ZnO30%	46.4	14.9	___	1.35	___	___	___	___	___	37.2
K-ZnO40%	39.2	15.02	___	___	___	___	___	2.66	___	43.07

TABLE 2. Thermodynamic parameters for TH photodegradation by K-ZnO under different temperatures.

K-ZnO				
T	K_a	ΔG°	Slope (ΔS°) KJ/k mol	intercept(ΔH°) KJ/ mol
333	**0.79**	**0.64**		
338	**0.93**	**0.21**	**0.08**	**25.9**
343	**1.04**	**-0.11**		

Effect of thermodynamics

The photodegradation of TH by (K-ZnO40%) was carried out at different temperatures at 12 mg L^{-1}initial concentration of TH. Free energy of photodegradation (ΔG°) was calculated from the following Eq. (3):

$$\Delta G = - RT \ln K \qquad (3)$$

where K is the equilibrium constant and T is the solution temperature, R is gas constant (8.314 J K^{-1} mol^{-1}). The enthalpy (ΔH°) and entropy (ΔS°) were calculated using the Van't Hoff Eq. (4).

$$\ln K = \frac{\Delta S}{R} - \frac{\Delta H}{R}\left(\frac{1}{T}\right) \qquad (4)$$

Photodegradation at different temperature is usually indicated the favorability of the degradation process. The effect of temperature on the TH degradation by ZnO nanoparticles has been studied. The obtained data shows that the degradation capacity has increased by increasing the temperature from 333 K to 343 K. **Fig. 10** shows the endothermic nature of TH degradation. Thermodynamic parameters such as, free energy change (ΔG°), enthalpy (ΔH°) and entropy (ΔS°) have evaluated to confirm the nature of degradation of TH by ZnO nanoparticles as mentioned in **Table 2**. The positive values of ΔH° and ΔS° show that the photodegradation process is endothermic by increasing the randomness of the system. The positive value of free energy indicates that the adsorption process is not spontaneous. Moreover, the value of free energy decreased with increasing temperature suggests that the photodegradation became more favorable at lower temperatures.

Conclusion

Simple and cheap method was used to prepare ZnO NPs. Kaolinite: ZnO ratio was optimized in order to reach the highest photocatalytic activity. The optimum ratio was found to be 40% ZnO/K. Moreover, the study offers a low cost technique to remove TH using photodegradation based on K/ZnO nanocomposite. The Photodegradation results of TH demonstrated that the high removal was found at pH 9. TH Photodegradation has been fulfilled using pseudo- first -order kinetic model rather than pseudo- second -order. Thermodynamic calculation has revealed that the Photodegradation of TH by K/ZnO40% is not spontaneous and the process is endothermic and photodegradaion became more favorable at lower temperatures. To conclude, the K/ZnO40% could be considered as an excellent candidate to

be used as photodcatalyst for the removal of TH in wastewater treatment plants.

References

1. Ghanbari, D., Salavati-Niasari, M., and Ghasemi-Kooch, M. A sonochemical method for synthesis of Fe3O4 nanoparticles and thermal stable PVA-based magnetic nanocomposite. *Journal of Industrial and Engineering Chemistry*, **20**(6), 3970-3974 (2014).

2. Kutláková, K. M., Tokarský, J., and Peikertová, P. Functional and eco-friendly nanocomposite kaolinite/ZnO with high photocatalytic activity. *Applied Catalysis B: Environmental*, **162**, 392-400 (2015).

3. Yang, J., Zheng, J., Zhai, H., Yang, X., Yang, L., Liu, Y., and Gao, M. Oriented growth of ZnO nanostructures on different substrates via a hydrothermal method. *Journal of Alloys and Compounds*, **489**(1), 51-55 (2010).

4. Khaorapapong, N., Khumchoo, N., and Ogawa, M. Preparation of zinc oxide–montmorillonite hybrids. *Materials Letters*, **65**(4), 657-660 (2011)..

5. Li, J. H., Hong, R. Y., Li, M. Y., Li, H. Z., Zheng, Y., and Ding, J. Effects of ZnO nanoparticles on the mechanical and antibacterial properties of polyurethane coatings. *Progress in Organic Coatings*, **64**(4), 504-509 (2009).

6. Chandraboss, V. L., Natanapatham, L., Karthikeyan, B., Kamalakkannan, J., Prabha, S., and Senthilvelan, S. Effect of bismuth doping on the ZnO nanocomposite material and study of its photocatalytic activity under UV-light. *Materials Research Bulletin*, **48**(10), 3707-3712 (2013).

7. Sharma, B. K., Gupta, A. K., Khare, N., Dhawan, S. K., and Gupta, H. C. Synthesis and characterization of polyaniline–ZnO composite and its dielectric behavior. *Synthetic Metals*, **159**(5-6), 391-395 (2009).

8. Fatimah, I., Wang, S., and Wulandari, D. ZnO/montmorillonite for photocatalytic and photochemical degradation of methylene blue. *Applied Clay Science*, **53**(4), 553-560 (2011).

9. Wahab, R., Kim, Y. S., Hwang, I. H., and Shin, H. S. A non-aqueous synthesis, characterization of zinc oxide nanoparticles and their interaction with DNA. *Synthetic Metals*, **159**(23-24), 2443-2452 (2009).

10. Sebők, D., Szendrei, K., Szabó, T., and Dékány, I. Optical properties of zinc oxide ultrathin hybrid films on silicon wafer prepared by layer-by-layer method. *Thin Solid Films*, **516**(10), 3009-3014 (2008).

11. Pudukudy, M., and Yaakob, Z. Facile solid state synthesis of ZnO hexagonal nanogranules with excellent photocatalytic activity. *Applied Surface Science*, **292**, 520-530 (2014).

12. Shifu, C., Wei, Z., Sujuan, Z., and Wei, L. Preparation, characterization and photocatalytic activity of N-containing ZnO powder. *Chemical Engineering Journal*, **148**(2-3), 263-269 (2009).

13. Ananthakumar, S., Anas, S., Ambily, J., and Mangalaraja, R. V. Microwave assisted citrate gel combustion synthesis of ZnO part-II: assessment of functional properties. *J Ceram Process Res*, **11**(2), 164-169 (2010).

14. Liu, J., Chen, X., Wang, W., Liu, Y., Huang, Q., and Guo, Z. Self-assembly of [101 [combining macron] 0] grown ZnO nanowhiskers with exposed reactive (0001) facets on hollow spheres and their enhanced gas sensitivity. *Cryst. Eng. Comm.*, **13**(10), 3425-3431 (2011).

15. Saikia, N. J., Bharali, D. J., Sengupta, P., Bordoloi, D., Goswamee, R. L., Saikia, P. C., and Borthakur, P. C. Characterization, beneficiation and utilization of a kaolinite clay from Assam, India. *Applied Clay Science*, **24**(1-2), 93-103 (2003).

16. Alkan, M., Demirbaş, Ö., and Doğan, M. Adsorption kinetics and thermodynamics of an anionic dye onto sepiolite. *Microporous and Mesoporous Materials*, **101**(3), 388-396 (2007).

17. Vimonses, V., Lei, S., Jin, B., Chow, C. W., and Saint, C. Adsorption of congo red by three Australian kaolins. *Applied Clay Science*, **43**(3-4), 465-472 (2009).

18. Clarot, F., Goulle, J. P., Vaz, E., and Proust, B. Fatal overdoses of tramadol: is benzodiazepine a risk factor of lethality?. *Forensic Science International*, **134**(1), 57-61 (2003).

19. Rúa-Gómez, P. C., and Püttmann, W. Occurrence and removal of lidocaine, tramadol, venlafaxine, and their metabolites in German wastewater treatment plants. *Environmental Science and Pollution Research*, **19**(3), 689-699 (2012).

20. Eawag, Screening measurements of organic micro-pollutants in lake Constance, (2009). http://www.eawag.ch/organisation/abteilungen/uchem/schwerpunkte/projektuebersicht/pojekt41/schlussbericht_bodensee.pdf (in German)

21. Kasprzyk-Hordern, B., Dinsdale, R. M., and Guwy, A. J. The occurrence of pharmaceuticals, personal care products, endocrine disruptors and illicit drugs in surface water in South Wales, UK. *Water Research*, **42**(13), 3498-3518 (2008).

22. Spiller, H. A., Gorman, S. E., Villalobos, D., Benson, B. E., Ruskosky, D. R., Stancavage, M. M., and Anderson, D. L. Prospective multicenter evaluation of tramadol exposure. *Journal of Toxicology: Clinical Toxicology,* **35**(4), 361-364 (1997).

23. Mohammadi, Z., Sharifnia, S., and Shavisi, Y. Photocatalytic degradation of aqueous ammonia by using TiO2ZnO/LECA hybrid photocatalyst. *Materials Chemistry and Physics*, **184**, 110-117 (2016).

24. Omar, F. M., Aziz, H. A., and Stoll, S. Aggregation and disaggregation of ZnO nanoparticles: influence of pH and adsorption of Suwannee River humic acid. *Science of the Total Environment*, **468**, 195-201 (2014).

25. Ali, M. E., El-Aty, A. M. A., Badawy, M. I., and Ali, R. K. Removal of pharmaceutical pollutants from synthetic wastewater using chemically modified biomass of green alga Scenedesmus obliquus. *Ecotoxicology and Environmental Safety*, **151**, 144-152 (2018).

26. Lambropoulou, D., Evgenidou, E., Saliverou, V., Kosma, C., and Konstantinou, I. Degradation of venlafaxine using TiO2/UV process: kinetic studies, RSM optimization, identification of transformation products and toxicity evaluation. *Journal of Hazardous Materials*, **323**, 513-526 (2017).

27. Eskizeybek, V., Sarı, F., Gülce, H., Gülce, A., and Avcı, A. Preparation of the new polyaniline/ZnO nanocomposite and its photocatalytic activity for degradation of methylene blue and malachite green dyes under UV and natural sun lights irradiations. *Applied Catalysis B: Environmental*, **119**, 197-206 (2012).

28. Yang W., Wu D., Fu R. Effect of surface chemistry on the adsorption of basic dyes on carbon aerogels. *Colloid Surf. A: Physicochem. Eng. Aspects* **312**, 118–124 (2008).

29. Niu, J., Zhang, L., Li, Y., Zhao, J., Lv, S., and Xiao, K. Effects of environmental factors on sulfamethoxazole photodegradation under simulated sunlight irradiation: Kinetics and mechanism. *Journal of Environmental Sciences*, **25**(6), 1098-1106 (2013).

30. Yang, H., Li, G., An, T., Gao, Y., and Fu, J. Photocatalytic degradation kinetics and mechanism of environmental pharmaceuticals in aqueous suspension of TiO2: A case of sulfa drugs. *Catalysis Today*, **153**(3-4), 200-207 (2010).

31. Pare, B., Jonnalagadda, S. B., Tomar, H., Singh, P., and Bhagwat, V. W. ZnO assisted photocatalytic degradation of acridine orange in aqueous solution using visible irradiation. *Desalination*, **232**(1-3), 80-90 (2008).

32. Li, Z., Hong, H., Liao, L., Ackley, C. J., Schulz, L. A., MacDonald, R. A. and Emard, S. M. A mechanistic study of ciprofloxacin removal by kaolinite. *Colloids and Surfaces B: Biointerfaces*, **88**(1), 339-344 (2011).

33. Rakić, V., Rajić, N., Daković, A., and Auroux, A. The adsorption of salicylic acid, acetylsalicylic acid and atenolol from aqueous solutions onto natural zeolites and clays: Clinoptilolite, bentonite and kaolin. *Microporous and Mesoporous Materials*, **166**, 185-194 (2013).